

Infrared Spectrum of the Hyponitrite Dianion, $\text{N}_2\text{O}_2^{2-}$, Isolated and Insulated from Stabilizing Metal Cations in Solid Neon

Lester Andrews,* Xuefeng Wang, Mingfei Zhou, and Binyong Liang

University of Virginia, Department of Chemistry, Charlottesville, Virginia 22904-4319

Received: August 17, 2001; In Final Form: October 23, 2001

Co-deposition of laser-ablated metals with NO in excess neon at 4 K produced new 1060.8 ± 0.4 and $1052.6 \pm 0.2 \text{ cm}^{-1}$ absorptions, which almost disappear on annealing to 9 K and reappear in part on ultraviolet irradiation. These absorptions shift with $^{15}\text{N}^{16}\text{O}$ and $^{15}\text{N}^{18}\text{O}$ substitution as fundamental N–O vibrations and exhibit 1:2:1 triplet bands with $^{14}\text{N}^{16}\text{O} + ^{15}\text{N}^{16}\text{O}$ and $^{15}\text{N}^{16}\text{O} + ^{15}\text{N}^{18}\text{O}$ mixtures, which demonstrates the involvement of two equivalent NO oscillators. The above absorptions are assigned to $\text{N}_2\text{O}_2^{2-}$ isolated and insulated from metal stabilizing cations in two solid neon matrix configurations. The blue shift from the 1028.5 cm^{-1} solid argon band position for this species is larger than found for most small molecules and anions, which is consistent with a dianion. The photochemistry in laser-ablated gold experiments suggests the involvement of N_2O_2^- in electron-transfer processes to form $\text{N}_2\text{O}_2^{2-}$.

Introduction

Although most atoms and many small molecules form stable monoanions,¹ only recently has evidence for isolated dianions become available.^{2–9} The stable isolated dianions are large enough to allow the two extra electrons to be separated and minimize coulomb repulsion. Many dianions are short-lived: the BeF_4^{2-} and MgF_4^{2-} dianions have lifetimes in the 10^{-4} s range,¹⁰ and new short-lived resonance states of NO_2^{2-} are estimated to have much shorter lifetimes on the order of 10^{-16} s.¹¹ The isolated sulfate dianion is unstable, but three water molecules are sufficient to stabilize a free SO_4^{2-} dianion, and sulfate dianions are abundant in ionic solids.¹²

Using the matrix isolation technique and laser-ablation of group 1 and 2 metals as a source of cations and electrons, we recently reported the infrared spectrum of $\text{N}_2\text{O}_2^{2-}$ isolated and insulated from stabilizing metal cations in solid argon.¹³ In these experiments, a new metal independent 1028.5 cm^{-1} absorption with isotopic substitution behavior for an N_2O_2 species was identified as $\text{N}_2\text{O}_2^{2-}$ formed by electron attachments to $(\text{NO})_2$ and $(\text{NO})_2^-$. The observation below N_2O_2^- at 1222 cm^{-1} in solid argon¹⁴ and proximity to the strong 1030 cm^{-1} infrared band^{15–17} for solid $\text{Na}_2\text{N}_2\text{O}_2$ substantiated this assignment. We report here the complementary observation of $\text{N}_2\text{O}_2^{2-}$ in solid neon using transition and actinide metals, which further characterizes the isolated $\text{N}_2\text{O}_2^{2-}$ dianion species.

Experimental Section

The experiment for laser ablation and matrix isolation has been described in detail previously.^{18,19} The Nd:YAG laser fundamental (1064 nm, 10 Hz repetition rate with 10 ns pulse width) was focused on rotating metal targets (Johnson-Matthey). Laser energies ranging from 1 to 40 mJ/pulse were used. Laser-ablated metal atoms, cations, and electrons were co-deposited with nitric oxide at 0.1–0.3% in neon onto 4–5 K CsI window at 2–4 mmol/h for 30 min to 1h using an old APD Cryogenics Heliplex or a new Sumitomo Heavy Industries Model RDK-205D Cryocooler. Several isotopic samples ($^{14}\text{N}^{16}\text{O}$, Matheson; $^{15}\text{N}^{16}\text{O}$, MDS isotopes, 99%; $^{15}\text{N}^{18}\text{O}$, Isotec, 99%, ^{15}N , 98%

^{18}O ; $^{14}\text{NO} + ^{15}\text{NO}$ mixtures; $^{15}\text{N}^{16}\text{O} + ^{15}\text{N}^{18}\text{O}$ mixtures) were used. Infrared spectra were recorded at 0.5 cm^{-1} resolution on a Nicolet 750 spectrometer with 0.1 cm^{-1} accuracy with a HgCdTe detector. Experiments were also performed with 10% as much CCl_4 as NO in order to capture electrons and alter the product yield.^{20–23} Matrix samples were annealed at a range of temperatures (6–12 K, neon) and subjected to broadband photolysis by a medium-pressure mercury arc (Philips, 175 W) with the globe removed ($\lambda > 240 \text{ nm}$).

Results and Discussion

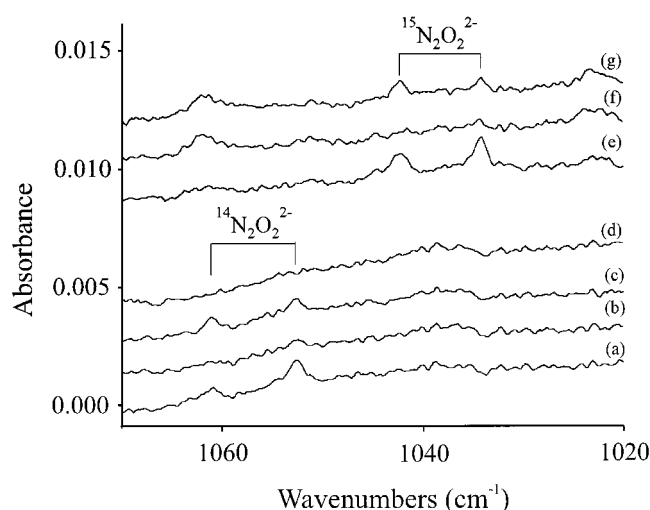
New neon matrix absorptions observed in laser-ablated metal experiments with NO will be identified by isotopic substitution, photochemical behavior, and comparison to argon matrix observations.¹³ Table 1 lists most of the absorptions common to these experiments that have been identified previously, in particular the charged species.^{24,25}

New Neon Matrix Absorptions. Weak new bands were observed at 1061.0 and 1052.6 cm^{-1} after deposition of laser-ablated Sc and Ti with NO in excess neon at 4 K. Figure 1 shows these bands, their demise on annealing to 9 K, and their partial regeneration on broadband $\lambda > 240 \text{ nm}$ irradiation. Note that the 1061.0 cm^{-1} band is favored relative to the 1052.6 cm^{-1} band on irradiation. A further 9 K annealing again destroys these absorptions. The same bands were observed in a second experiment, and it was noted that the intensity decreased with time of exposure to the glower source. The intensity was maximum after 64 scans, and after five sets of 64 scans, the signal was gone. However, 240–380 nm irradiation regenerated the bands with slightly more intensity than that in Figure 1a, and 9 K annealing destroyed them as before. In a vanadium experiment, the two bands were observed on sample deposition and destroyed by an immediate $\lambda > 850 \text{ nm}$ irradiation using a low-intensity tungsten lamp. The ^{15}NO counterparts at 1042.3 and 1034.2 cm^{-1} exhibited similar behavior (Figure 1e–g).

The 1061.0 and 1052.6 cm^{-1} absorptions were eliminated by CCl_4 doping in a scandium experiment where $(\text{NO})_2^+$ increased by 50% and $(\text{NO})_2^-$ decreased by 80%. In some

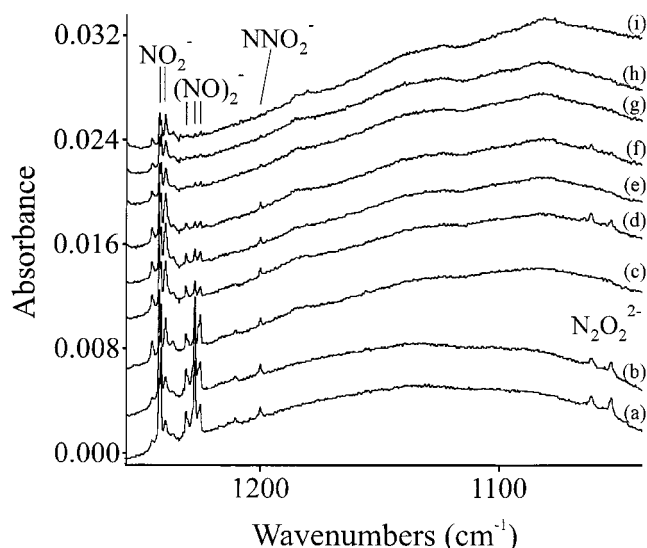
TABLE 1: Infrared Absorptions (cm^{-1}) Observed for Reactions of Laser-Ablated Late Transition Metals with NO in Excess Neon at 4 K

$^{14}\text{N}^{16}\text{O}$	$^{15}\text{N}^{16}\text{O}$	$^{15}\text{N}^{18}\text{O}$	14–16/15–16	15–16/15–18	identification
1874.4	1841.4	1791.8	1.0179	1.0277	NO
1866.3	1833.4	1784.1	1.0179	1.0276	<i>cis</i> -(NO) ₂
1857.8	1824.9	1775.6	1.0180	1.0278	NO site
1780.4	1748.8	1701.6	1.0181	1.0277	<i>cis</i> -(NO) ₂
1760.5	1729.9	1683.7	1.0177	1.0274	<i>trans</i> -(NO) ₂
1619.0	1591.1	1548.4	1.0175	1.0276	(NO) ₂ ⁺
1424.1	1399.3	1362.4	1.0177	1.0271	(NO) ₂ ⁺
1369.9	1346.4	CH ₄	1.0174		(NO) ₃ ⁻
1242.2	1216.9	1190.6	1.0208	1.0221	NO ₂ ⁻
1239.8	1214.3	1188.3	1.0210	1.0219	NO ₂ ⁻ site
1230.9	1209.7	1176.8	1.0175	1.0279	<i>trans</i> -(NO) ₂ ⁻ site
1227.3	1206.1	1173.5	1.0176	1.0278	<i>trans</i> -(NO) ₂ ⁻
1225.1	1200.9	1174.2	1.0202	1.0227	<i>cis</i> -(NO) ₂ ⁻
1199.8	1176.2	1150.5	1.0201	1.0223	NNO ₂ ⁻
1060.6	1042.2	1014.3	1.0177	1.0275	N ₂ O ₂ ²⁻ site
1052.4	1034.1	1006.4	1.0177	1.0275	N ₂ O ₂ ²⁻

**Figure 1.** Infrared spectra in the 1070–1020 cm^{-1} region for laser-ablated scandium and NO in excess neon at 4 K: 0.2% $^{14}\text{N}^{16}\text{O}$ in neon co-deposited (a) for 60 min, (b) after annealing to 9 K, (c) after $\lambda > 240$ nm irradiation, and (d) after annealing to 9 K; 0.2% $^{15}\text{N}^{16}\text{O}$ in neon co-deposited (e) for 60 min, (f) after annealing to 9 K, and (g) after $\lambda > 240$ nm irradiation.

experiments, the 1052.6 cm^{-1} feature is stronger after 30 min sample deposition than that after 60 min, which indicates a photosensitive species. After 30 min deposition in a Y experiment, the signals were strongest in the initial spectrum recorded with 64 scans, and the intensity decreased in successive 64-scan spectra until the background noise level was reached after recording five 64-scan spectra; the same effect was found in the argon matrix investigation.¹³ Similar behavior was observed for weak 1061.0 and 1052.6 cm^{-1} bands in experiments with Li and Na in solid neon. Analogous bands were observed with Y and La at 1061.0 and 1052.4 cm^{-1} , 1042.2 and 1034.0 cm^{-1} , and 1013.9 and 1006.4 cm^{-1} using $^{14}\text{N}^{16}\text{O}$, $^{15}\text{N}^{16}\text{O}$, and $^{15}\text{N}^{18}\text{O}$, respectively.

Earlier experiments with U gave unreported absorptions at 1060.8 and 1052.5 cm^{-1} ($A = 0.0010$), which disappeared on annealing to 8 K (Figure 1 of ref 26); ^{15}NO counterparts were observed at 1042.5 and 1034.2 cm^{-1} . These new absorptions were produced when a cold Ne/NO sample was subjected separately to the radiation from laser-excited uranium (not shown in Figure 3 of ref 26). The associated Th investigation produced slightly different 1060.4 and 1052.4 cm^{-1} ($A = 0.0012$) absorptions, which disappeared on annealing to 8 K;

**Figure 2.** Infrared spectra in the 1260–1040 cm^{-1} region for laser-ablated gold and NO in excess neon at 4 K: 0.2% $^{14}\text{N}^{16}\text{O}$ in neon co-deposited (a) for 30 min, 128 scans, (b) for 128 more scans, (c) after 9 K annealing, (d) after 240–380 nm irradiation, (e) after $\lambda > 370$ nm irradiation, (f) after 240–380 irradiation, (g) after $\lambda > 240$ nm irradiation, (h) after 240–380 nm irradiation, and (i) after annealing to 9 K.

$^{15}\text{N}^{16}\text{O}$ counterparts (1041.9, 1034.1 cm^{-1}) and $^{15}\text{N}^{18}\text{O}$ analogues (1014.2, 1006.4 cm^{-1}) were observed, and a mixture of the latter gave triplets with new intermediate bands at 1027.5 and 1019.8 cm^{-1} . These absorptions were also observed when a cold Ne/NO sample was subjected to laser-excited thorium radiation.

Experiments with gold are particularly informative: the subject bands observed on deposition at 1061.1–1060.8 and 1052.7–1052.4 cm^{-1} depended on concentration of NO and laser energy, which determines the metal concentration. Infrared spectra are illustrated in Figure 2: the new absorptions at 1061.1 and 1052.7 cm^{-1} are stronger after 128 scans than after a second immediate set of 128 scans, but the NO_2^- , $(\text{NO})_2^-$, and NNO_2^- absorptions are not affected by the infrared source radiation. The new absorptions are destroyed by 9 K annealing, which increases $(\text{NO})_2$. A subsequent 240–380 nm irradiation partly restores the new absorptions favoring the upper band and decreases $(\text{NO})_2^-$ and $(\text{NO})_2$ bands. Visible photolysis ($\lambda > 380$ nm) destroys the new bands with little obvious change elsewhere. Subsequent $\lambda > 240$ nm and 240–380 nm irradiations decreased the NO_2^- , $(\text{NO})_2^-$, and NNO_2^- absorptions but failed to restore the new absorptions.

Infrared spectra from neon matrix experiments with Fe, Co, Ni, and Cu reported earlier^{22,23} revealed weak bands ($A = 0.0005$) in the 1000 cm^{-1} region, as listed in Table 1. These bands disappeared on annealing to 6 and 8 K and were not regenerated on broadband mercury arc irradiation. Doping with CCl_4 in the Ni experiment eliminated the 1060.6 and 1052.4 cm^{-1} bands and reduced NO_2^- and $(\text{NO})_2^-$ and increased $(\text{NO})_2^+$ absorptions. In addition to the $^{14}\text{N}^{16}\text{O}$, $^{15}\text{N}^{16}\text{O}$, and $^{15}\text{N}^{18}\text{O}$ isotopic bands, mixed isotopic samples gave triplet patterns for each mixture as illustrated in Figure 3 for laser-ablated cobalt. The two triplet systems overlap for the $^{14}\text{N}^{16}\text{O} + ^{15}\text{N}^{16}\text{O}$ mixture and the 1051.5 cm^{-1} $^{14}\text{N}^{16}\text{O} + ^{15}\text{N}^{16}\text{O}$ component for the upper triplet falls on the 1052.4 cm^{-1} $^{14}\text{N}^{16}\text{O}$ absorption, while the stronger mixed isotopic component for the lower triplet at 1043.0 cm^{-1} masks the 1042.2 cm^{-1} $^{15}\text{N}^{16}\text{O}$ absorption. The two triplet systems are resolved for the $^{15}\text{N}^{16}\text{O}$

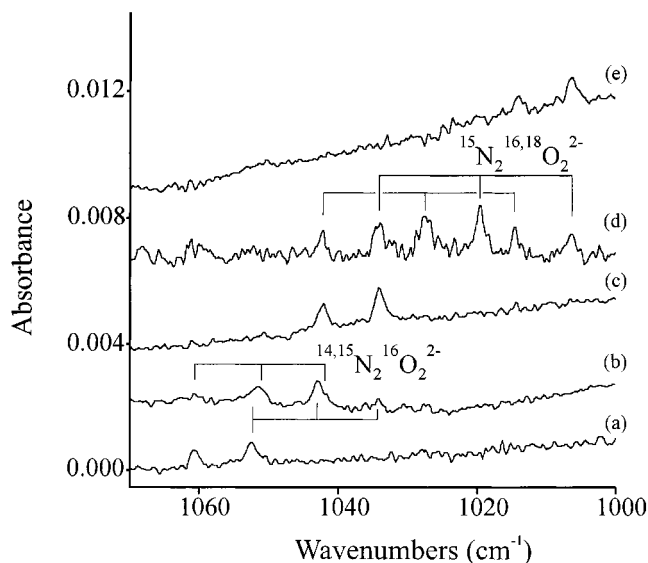


Figure 3. Infrared spectra in the 1070–1000 cm^{-1} region for laser-ablated cobalt and NO in excess neon at 4 K: (a) 0.1% $^{14}\text{N}^{16}\text{O}$ in neon co-deposited for 30 min, (b) 0.05% $^{14}\text{N}^{16}\text{O}$ + 0.05% $^{15}\text{N}^{16}\text{O}$, (c) 0.1% $^{15}\text{N}^{16}\text{O}$, (d) 0.05% $^{15}\text{N}^{16}\text{O}$ + 0.05% $^{15}\text{N}^{18}\text{O}$, and (e) 0.1% $^{15}\text{N}^{18}\text{O}$.

+ $^{15}\text{N}^{18}\text{O}$ mixture, and mixed isotopic bands are observed at 1027.4 and 1019.6 cm^{-1} for each isotopic triplet.

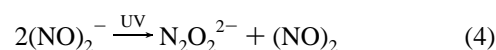
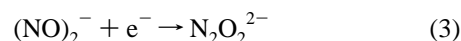
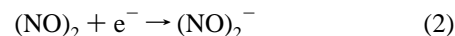
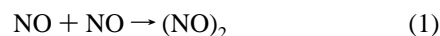
Identification of the 1060.8 ± 0.4 and 1052.6 ± 0.2 cm^{-1} Absorptions.

The isotopic data (Table 1) show that these absorptions are due to a fundamental N–O stretching mode as the 14–16/15–16 and 15–16/15–18 isotopic frequency ratios are virtually unchanged from those of NO itself. Furthermore, the 1:2:1 triplet patterns with mixed isotopic precursors demonstrate that the vibrational mode involves two equivalent NO subunits. Following the neon matrix identification of $(\text{NO})_2^-$ near 1227 cm^{-1} , solid $\text{Ag}_2\text{N}_2\text{O}_2$ at 1058 cm^{-1} , solid $\text{Na}_2\text{N}_2\text{O}_2$ near 1030 cm^{-1} , and $\text{N}_2\text{O}_2^{2-}$ isolated in solid argon at 1028.5 cm^{-1} , the above new neon matrix bands are assigned to the $\text{N}_2\text{O}_2^{2-}$ dianion isolated in solid neon.^{13–17,24} The slight variation in band position in different experiments is in part due to asymmetric band profile as well as the concentration of reagent species. Since the metal cation Coulomb field is required to stabilize the dianion, some small metal dependence for the dianion is reasonable.

What information does the observation of $\text{N}_2\text{O}_2^{2-}$ in solid neon at 1060.8 and 1052.6 cm^{-1} , blue-shifted from the 1028.5 cm^{-1} solid argon value, provide to help understand the dianion species? The blue matrix shift (32 and 24 cm^{-1}) from argon to neon is much larger than the 2.4 and 6.3 cm^{-1} blue shifts observed for *cis*- and *trans*- $(\text{NO})_2^-$ and the 4.2 cm^{-1} blue shift observed for *cis*- $(\text{NO})_2$. This is consistent with the expected greater difference between the argon and neon electrostatic interaction for the more polarizable dianion.

The internal electrostatic repulsion must be reduced to a minimum in order to stabilize the dianion, and the Coulomb field of the metal cations trapped in the solid neon matrix help accomplish this by attracting negative charge to the oxygen ends of the dianion as suggested by the $(\text{M}^+(\text{Ne})(\text{O}^--\text{N}=\text{N}-\text{O}^-)-(\text{Ne})(\text{M}^+))$ representation. The N–N bond energy in $(\text{NO})_2$ is 1–2 kcal/mol, but this increases to 30 kcal/mol in $(\text{NO})_2^-$ on the basis of experimental measurement and theoretical calculations.^{27,28} The decrease in antisymmetric N–O stretching frequency from 1780 cm^{-1} for $(\text{NO})_2$ to 1227 cm^{-1} for $(\text{NO})_2^-$ to 1052 cm^{-1} for $(\text{NO})_2^{2-}$ arises from a decrease in N–O bond strength, which is accompanied by an increase in N–N bond strength in the series.

Reactions in the Matrix. The $\text{N}_2\text{O}_2^{2-}$ dianion isolated in solid neon is conceptually the same as the dianion in solid argon: the dianion is stabilized by the Coulomb field of metal cations in the matrix separated by at least one neon diameter from the dianion (see Scheme 1 in ref 13). Atomic gold has an ionization energy (212 kcal/mol, 134 nm) far too high to yield photoelectrons using $\lambda > 240$ nm radiation, which was postulated to account for the photochemical formation of $\text{N}_2\text{O}_2^{2-}$ in an argon matrix sample containing Li (or Na) and $(\text{NO})_2$.¹³ The $(\text{NO})_2^-$ and $\text{N}_2\text{O}_2^{2-}$ anions are formed here during laser-ablation of metals and co-deposition of M, M^+ , e^- , and NO in excess neon by reactions 1, 2, and 3. Annealing the neon matrix



to 9 K allows diffusion of trapped species and neutralization of all of the more vulnerable $\text{N}_2\text{O}_2^{2-}$ species and some $(\text{NO})_2^-$. Irradiation with UV light (240–380 nm) restores the $\text{N}_2\text{O}_2^{2-}$ signal at the expense of about 70% of the $(\text{NO})_2^-$ absorbance (Figure 2d). This suggests that UV radiation initiates photoelectron reaction 4 and forms $\text{N}_2\text{O}_2^{2-}$ at a rate faster than $\text{N}_2\text{O}_2^{2-}$ is destroyed. However, visible light irradiation efficiently destroys the $\text{N}_2\text{O}_2^{2-}$ signal with little change of the $(\text{NO})_2^{2-}$ absorptions (Figure 2e); the visible photodestruction of $\text{N}_2\text{O}_2^{2-}$ probably goes all the way back to $(\text{NO})_2$, but the $(\text{NO})_2$ absorption is too strong to measure small changes in absorbance. A subsequent UV irradiation produces $\text{N}_2\text{O}_2^{2-}$ with reduced yield as most of the $(\text{NO})_2^-$ precursor has been depleted (Figure 2f).

The $\text{N}_2\text{O}_2^{2-}$ species is also formed along with $(\text{NO})_2^-$ and $(\text{NO})_2^+$ when cold solid Ne/NO matrix samples were irradiated by emission from laser-ablated Th and U.²⁶ This shows that electrons produced in photoionization processes undergo successive reactions 2 and 3 to form $\text{N}_2\text{O}_2^{2-}$ and provides further support for the present identification of the $\text{N}_2\text{O}_2^{2-}$ dianion in solid neon.

Conclusions

Co-deposition of laser-ablated transition and actinide metals with NO in excess neon at 4 K produced new 1060.8 ± 0.4 and 1052.6 ± 0.2 cm^{-1} absorptions, which almost disappear on annealing to 9 K. Although this new species is extremely sensitive to visible light, it reappears in part on ultraviolet irradiation. These absorptions shift with $^{15}\text{N}^{16}\text{O}$ and $^{15}\text{N}^{18}\text{O}$ substitution as fundamental N–O vibrations and exhibit 1:2:1 triplet bands with $^{14}\text{N}^{16}\text{O} + ^{15}\text{N}^{16}\text{O}$ and $^{15}\text{N}^{16}\text{O} + ^{15}\text{N}^{18}\text{O}$ mixtures, which demonstrates the involvement of two equivalent NO oscillators. The above absorptions are assigned to $\text{N}_2\text{O}_2^{2-}$ isolated and insulated from stabilizing metal cations in two solid neon matrix configurations. The blue shift from the 1028.5 cm^{-1} solid argon band position for this species is larger than that found for most small molecules and anions, which is consistent with a more polarizable dianion. The photochemistry in laser-ablated gold experiments suggests the involvement of N_2O_2^- in electron-transfer processes to form $\text{N}_2\text{O}_2^{2-}$. Finally, the formation of $(\text{NO})_2^+$, $(\text{NO})_2^-$, and $\text{N}_2\text{O}_2^{2-}$ in a cold solid Ne/NO sample subjected to laser-excited U and Th emission shows that photoelectrons are critical reagents in these electron

attachment reactions and supports the identification of the $\text{N}_2\text{O}_2^{2-}$ dianion in solid neon.

Acknowledgment. We gratefully acknowledge support from NSF Grant CHE 00-78836.

References and Notes

- (1) Hotop, H.; Lineberger, W. C. *J. Phys. Chem. Ref. Data* **1985**, *14*, 731.
- (2) Scheller, M. K.; Compton, R. N.; Cederbaum, L. S. *Science* **1995**, *270*, 1160.
- (3) Boldyrev, A. I.; Gutowski, M.; Simons, J. *Acc. Chem. Res.* **1996**, *29*, 497.
- (4) Wang, L.-S.; Wang, X.-B. *J. Phys. Chem. A* **2000**, *104*, 1978, and references therein.
- (5) Wang, X.-B.; Wang, L.-S. *J. Chem. Phys.* **1999**, *111*, 4497.
- (6) Ding, C. F.; Wang, X. B.; Wang, L. S. *J. Phys. Chem. A* **1998**, *102*, 8633.
- (7) Wang, X.-B.; Wang, L.-S. *J. Am. Chem. Soc.* **2000**, *122*, 2339.
- (8) Wang, X.-B.; Wang, L.-S. *J. Phys. Chem. A* **2000**, *104*, 4429.
- (9) Wang, X.-B.; Nicholas, J. B.; Wang, L.-S. *J. Chem. Phys.* **2000**, *113*, 653.
- (10) Middleton, R.; Klein, J. *Phys. Rev. A* **1999**, *60*, 3515.
- (11) Andersen, L. H.; Bilodeau, R.; Jensen, M. J.; Neilsen, S. B.; Safvan, C. P.; Seiersen, K. *J. Chem. Phys.* **2001**, *114*, 147.
- (12) Wang, X.-B.; Nicholas, J. B.; Wang, L.-S. *J. Chem. Phys.* **2000**, *113*, 10837.
- (13) Andrews, L.; Liang, B. *J. Am. Chem. Soc.* **2001**, *123*, 1997.
- (14) Andrews, L.; Zhou, M. F.; Willson, S. P.; Kushto, G. P.; Snis, A.; Panas, I. *J. Chem. Phys.* **1998**, *109*, 177 (M + NO in argon), and references therein.
- (15) Kuhn, L.; Lippincott, E. R. *J. Am. Chem. Soc.* **1956**, *78*, 1820.
- (16) Miller, D. J.; Polydropoulos, C. N.; Watson, D. *J. Chem. Soc.* **1960**, 687. Hay-Motherwell, R. S.; Wilkinson, G.; Sweet, T. K. N.; Hursthouse, M. B. *J. Chem. Soc., Dalton Trans.* **1994**, 2221.
- (17) McGraw, G. E.; Bernitt, D. L.; Hisatsune, I. C. *Spectrochim. Acta* **1967**, *23A*, 25.
- (18) Burkholder, T. R.; Andrews, L. *J. Chem. Phys.* **1991**, *95*, 8697.
- (19) Hassanzadeh, P.; Andrews, L. *J. Phys. Chem.* **1992**, *96*, 9177.
- (20) Zhou, M. F.; Andrews, L. *J. Am. Chem. Soc.* **1998**, *120*, 11499 (Ni + CO in Ar).
- (21) Zhou, M. F.; Andrews, L. *J. Am. Chem. Soc.* **1998**, *120*, 13230 (Sc + CO₂).
- (22) Zhou, M. F.; Andrews, L. *J. Phys. Chem. A* **2000**, *104*, 3915 (Fe, Co, Ni + NO).
- (23) Zhou, M. F.; Andrews, L. *J. Phys. Chem. A* **2000**, *104*, 2618 (Cu + NO).
- (24) Andrews, L.; Zhou, M. F. *J. Chem. Phys.* **1999**, *111*, 6036 (M + NO in neon), and references therein.
- (25) Lugez, C. L.; Thompson, W. E.; Jacox, M. E.; Snis, A.; Panis, I. *J. Chem. Phys.* **1999**, *110*, 10345.
- (26) Zhou, M. F.; Andrews, L. *J. Chem. Phys.* **1999**, *111*, 11044 (U, Th + NO in neon).
- (27) McKellar, A. R.; Watson, J. K. G.; Howard, B. J. *Mol. Phys.* **1995**, *86*, 273.
- (28) Snis, A.; Panas, I. *J. Chem. Phys.* **1997**, *221*, 1.